

A Robust Wearable Antenna for In-Body Communications

Shuai-Chao Yang, Lin Li*, and Xiao-Wei Gu

Abstract—A flexible antenna with high robustness is presented for wireless body area networks (WBANs) in-body communications. The coplanar waveguide (CPW) fed hexagon slot structure is employed to obtain a wide bandwidth of 34.4%. A parasitic patch is used to enhance in-body gain to -3.36 dBi. With these advantages, the proposed antenna is insensitive to frequency shift and gain reduction caused by environmental changes. Besides, the proposed low-profile antenna on a flexible substrate is well fit for wearable applications.

1. INTRODUCTION

Due to people's increasing concern for their health, WBANs including implantable devices have become popular now. In such applications, wearable in-body antennas are designed to receive data from implanted devices [1–7]. For such applications, environmental changes exert greater impact on antenna performance, resulting in frequency shift and gain reduction. Therefore, robust wearable in-body antennas insensitive to environmental changes are highly desired for in-body design.

Generally, the antenna robustness can be improved by increasing bandwidth and gain. Many in-body antennas with wideband bandwidth were proposed in [1–3]. However, their high-profile did not fit for wearable applications. Slot [4, 5] and circularly polarized patch [6] were also utilized to construct in-body antennas. However, these antennas with narrow bandwidth cannot deal with frequency shift caused by environmental changes. Monopole in-body antennas were proposed in [7]. However, its bandwidth still required further widening. Consequently, flexible and low-profile in-body antennas with high robustness are highly desired for wearable applications.

This paper proposes a flexible in-body antenna with high robustness. The antenna structure and its theory are studied in Section 2. The impedance performance, transmission performance, bending sensitivity, and specific absorption rate (SAR) are discussed in Section 3. Finally, the advantages of this design are summarized in Section 4.

2. ANTENNA DESIGN

Figure 1(a) shows the proposed antenna on a 1.5 mm-thick EPDM rubber material with a relative permittivity of $\epsilon_r = 1.53$ and loss tangent angle of $\tan \delta = 0.02$. A CPW-fed hexagonal patch is used to excite a hexagonal slot facing the body. A parasitic patch on the top layer of the substrate is used as a reflective surface to improve the gain. A 4-layer human body model is placed under the antenna as shown in Figure 1(b). The phantom consists of three layers of human tissue, including 4 mm-height skin ($\epsilon_r = 38$, bulk conductivity $\delta = 1.3$), 4 mm-height fat ($\epsilon_r = 4.4$, $\delta = 0.08$), and 80 mm-height muscle ($\epsilon_r = 56$, $\delta = 2.33$).

The proposed antenna is developed from hexagonal slot antenna Ant1 in Figure 2. For the convenience of fabricating the antenna manually, a hexagonal slot antenna instead of circular one is

Received 17 July 2022, Accepted 9 September 2022, Scheduled 21 September 2022

* Corresponding author: Lin Li (lilin_door@hotmail.com).

The authors are with the School of Information Science and Engineering, Zhejiang Sci-Tech University, Hangzhou, Zhejiang, China.

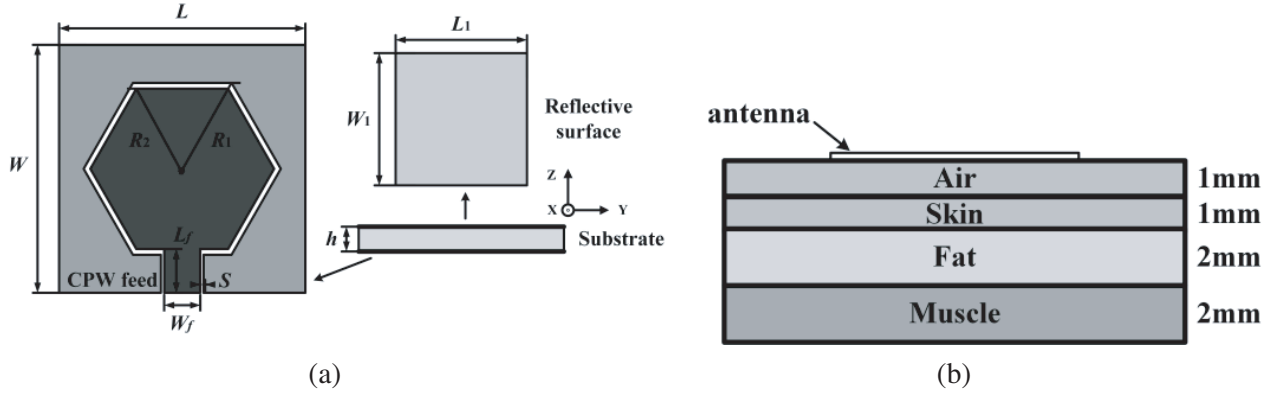


Figure 1. The proposed antenna configuration and simulation environment setup. (a) Antenna configuration. (b) Simulation environment setup.

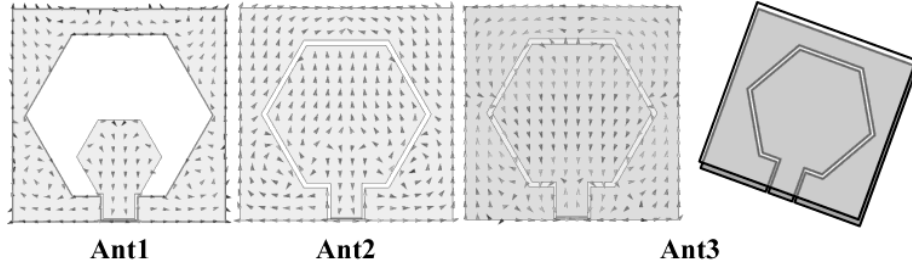


Figure 2. Evolution process from initial antenna to proposed antenna.

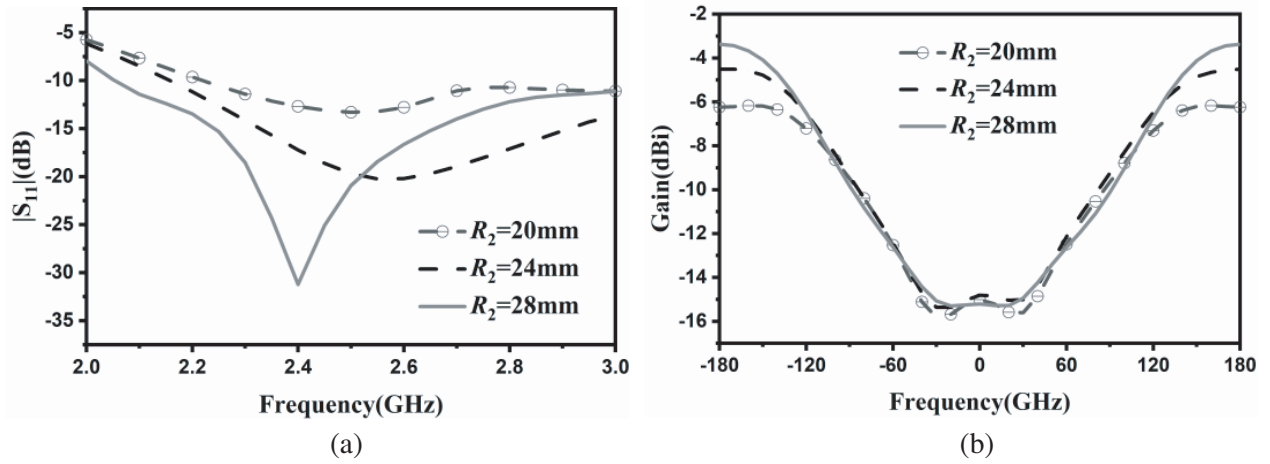


Figure 3. Simulated $|S_{11}|$ and gain with the change of antenna parameter R_2 . (a) $|S_{11}|$. (b) Gain.

adopted in this design. Though Ant1 has wide bandwidth, its gain is a little low, and it cannot meet the robust link requirement.

Consequently, Ant2 in Figure 2 is then developed by increasing the size of the hexagonal patch on the basis of Ant1. By doing this, the gain of its fundamental mode is effectively improved. To further investigate the influence of the hexagonal patch, Figure 3 compares simulated $|S_{11}|$ and gain with different R_2 . A larger R_2 helps to increase gain because larger R_2 leads to the enhancement of the field along the slot. However, the bandwidth decreases simultaneously. So R_2 should be adjusted properly to balance the bandwidth and gain.

To further increase gain, a parasitic patch is added on the top layer of the substrate to compose Ant3. Figure 4 compares simulated $|S_{11}|$ and gain with different parasitic patches. As shown in Figure 4, the antenna gain is increased since the parasitic patch reflects electromagnetic energy that escapes into free space. A larger $W_1 \times L_1$ leads to increased gain at the cost of larger size. So $W_1 \times L_1$ should also be chosen to balance the size and gain.

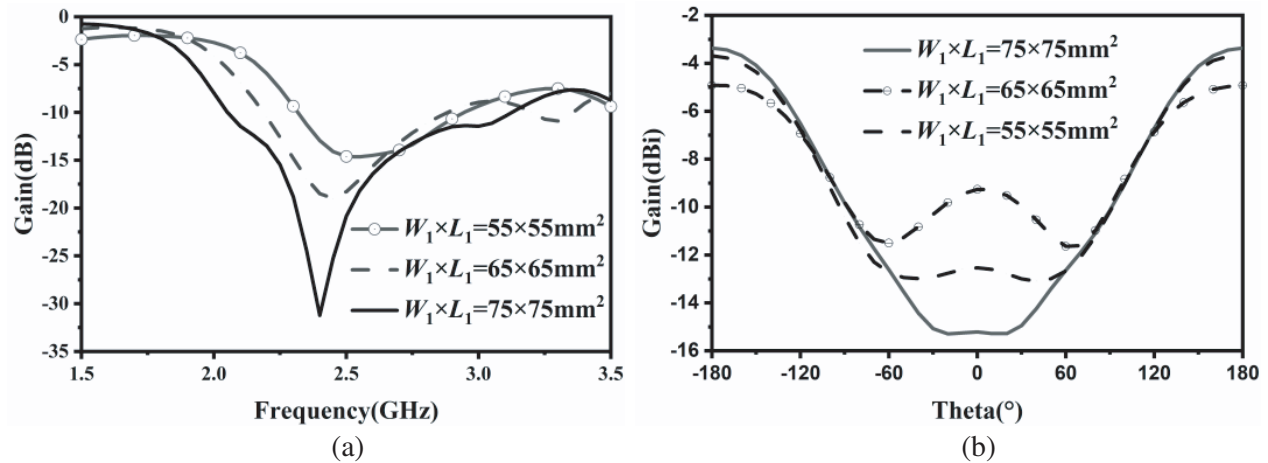


Figure 4. Simulated gain with the change of antenna parameter $W_1 \times L_1$. (a) $|S_{11}|$. (b) Gain.

Based on above procedure, the optimal dimensions of the antenna are obtained as follows: $W = W_1 = L = L_1 = 75 \text{ mm}$, $h = 1.5 \text{ mm}$, $s = 1 \text{ mm}$, $W_f = 11 \text{ mm}$, $L_f = 13.3 \text{ mm}$, $R_1 = 30 \text{ mm}$, $R_2 = 28 \text{ mm}$. The proposed antenna was fabricated by cutting and pasting $70 \mu\text{m}$ -thick copper foil tape on EPDM rubber. The contact resistance of copper foil tape is $0.005 \Omega/\text{m}^2$.

3. EXPERIMENTAL RESULTS

3.1. In-Body Performance and Discuss

To validate the in-body performance, reflection performance of the proposed antenna is firstly measured based on the measurement setup in Figure 5. Measured and simulated results are compared in Figure 6(a). A measured bandwidth of 34.4% is achieved for $|S_{11}|$ less than -10 dB (from 2.12 to

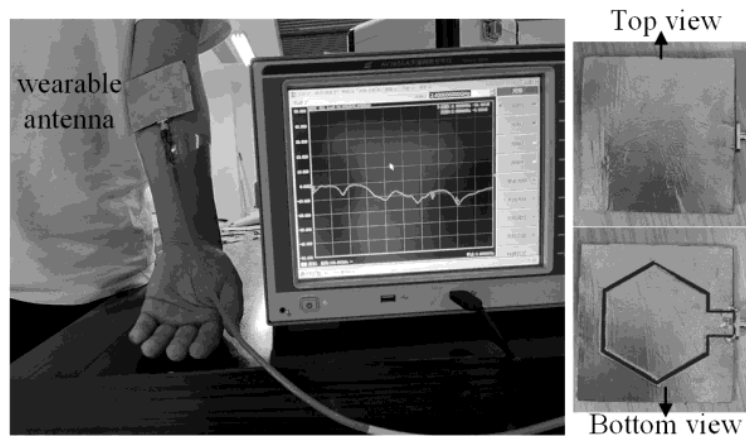


Figure 5. Measurement setup together with the fabricated antenna.

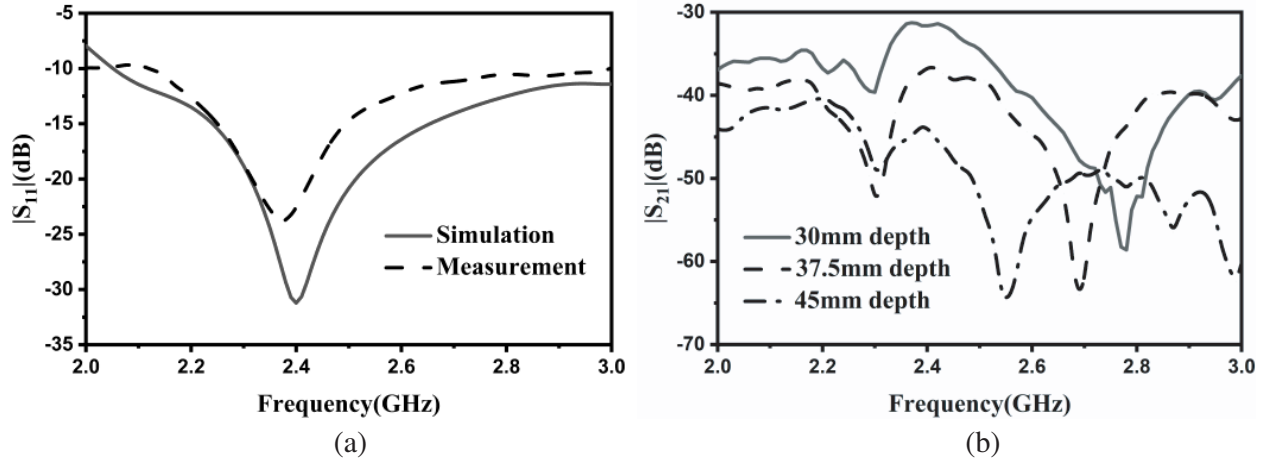


Figure 6. (a) Measured and simulated reflection coefficient $|S_{11}|$. (b) Measured $|S_{21}|$ between implantable antenna and this work for different implant depths.

3 GHz), while the simulated one of 41.4% is from 2.05 to 3.12 GHz. The discrepancies between the simulation and measurement are caused by fabricating errors and differences between the arm and the simulation model. Obviously, the antenna covers the WLAN frequency band with a wider bandwidth.

Transmission performance of the proposed antenna is evaluated through the measurements of transmission coefficient. An implantable antenna was used as the transmitting antenna, and this work was used as the receiving one. The measured $|S_{21}|$ between the implantable antenna and the proposed one is shown in Figure 6(b). The results show that this work achieves normal communication with the transceiver antenna of the implanted device and keeps stable communication when implantation depth varies from 30 to 45 mm.

To validate the robustness of the proposed antenna, Table 1 compares the proposed antenna with other in-body antennas in terms of operational frequency, profile height, relative bandwidth, gain, and transmission performance. The high-profile antennas in [1–3] are not suitable for wearable applications despite their wide bandwidth. As compared to other antennas [4–7], the proposed antenna has a wider -10 dB bandwidth, competitive gain, and transmission performance. So the proposed antenna exhibits higher robustness to environmental changes. Besides, the proposed low-profile antenna on a flexible substrate is more suitable for wearable communication than other rigid antennas [2–7].

Table 1. Comparison of in-body antennas in the references and the proposed one.

Reference	Frequency (GHz)	Substrate material	Profile height (mm)	Relative bandwidth (%)	Gain (dBi)	Peak $ S_{21} $ @depth (dB)
[1]	4	flexible	21	12.5	-4.98	-53.40@50 mm
[2]	6.5	rigidity	19	107.7	-	-5@50 mm
[3]	4.35	rigidity	13	53.8	-	-
[4]	2.4	rigidity	3.14	0.8	-	-37.4@60 mm
[5]	5.8	rigidity	10.5	7.2	-	-26@5 mm
[6]	2.4	rigidity	4.46	1.6	-	-56@75 mm
[7]	0.4	rigidity	0.64	21	-18	-24@9 mm
This work	2.4	flexible	1.5	34.4	-3.36	-31.38@30 mm

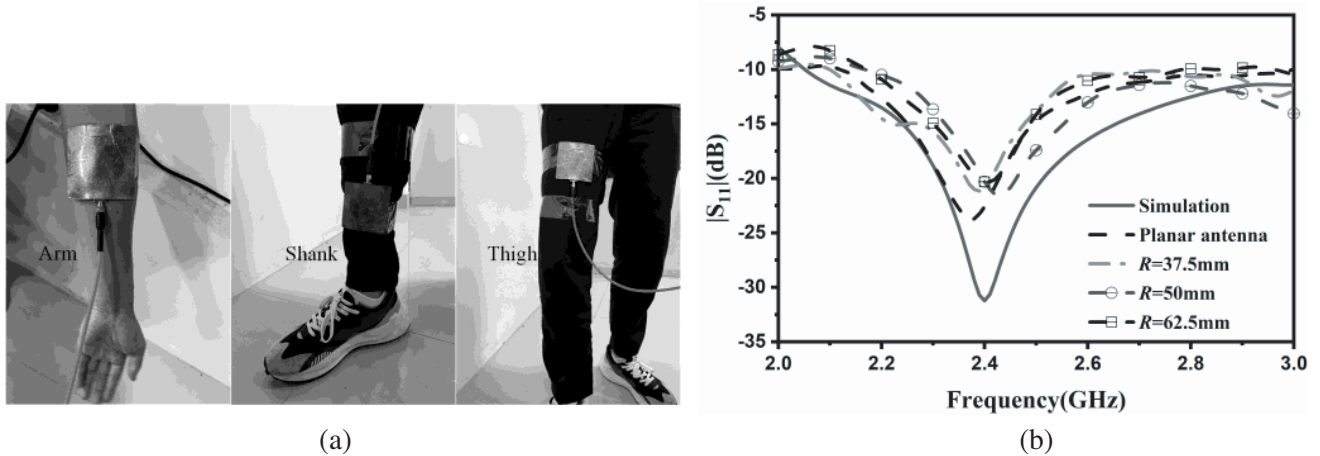


Figure 7. Bending measurement. (a) Setup. (b) Measurement for different bending.

3.2. Bending Effect

Bending effect on antenna performance is also validated. As shown in Figure 7(a), the antenna was bent and bound to the human body using transparent glue. The reflection coefficient of the antenna was measured on the human arm with a bending radius of 37.5 mm, on the shank with a bending radius of 50 mm, and on the thigh with a bending radius of 62.5 mm. The measured results are compared in Figure 7(b). The proposed antenna can cover WLAN band for any bending case. So the proposed antenna is insensitive to the bending.

3.3. SAR Situation

Assuming that the proposed antenna is placed at a height of 1 mm above the mannequin, SAR is simulated at the frequency where the minimum of $|S_{11}|$ occurs. As shown in Figure 8 SAR of the antenna is maximized around the slot. At an incident power of 30 mW, the 10 g average SAR of the antenna is 1.97 W/kg, which is in line with the 2 W/kg limit specified in Europe.

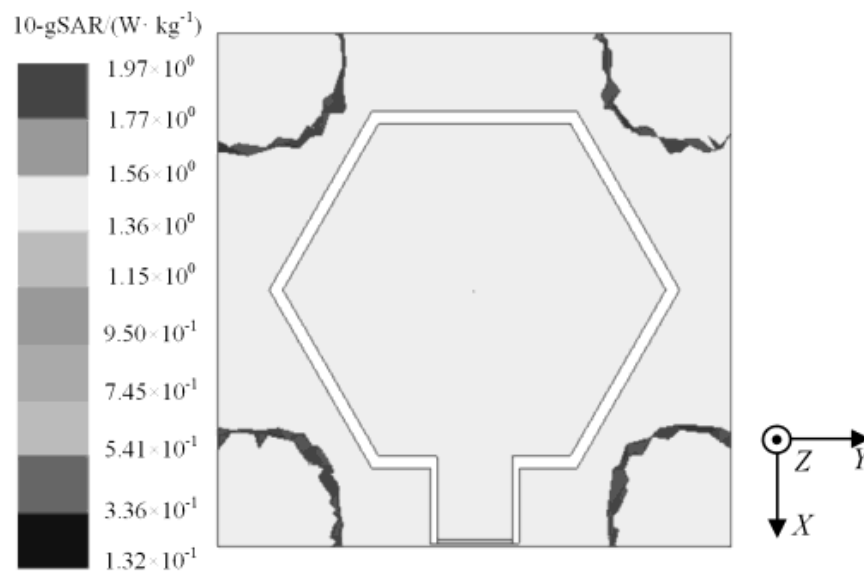


Figure 8. Simulated SAR distribution of the proposed antenna.

4. CONCLUSIONS

A wearable in-body antenna with high robustness to environmental changes is proposed for WBANs applications. The antenna has a measured bandwidth of 34.4% and an in-body gain of -3.36 dBi. The antenna is insensitive to bending, thus shows that the proposed antenna has higher robustness than other in-body antennas. Its low-profile flexible configuration makes it beneficial for wearable applications.

ACKNOWLEDGMENT

This work was supported by the State Key Laboratory of Laser-Material Interaction Development Fundamental Research Project (SKLLIM2113).

REFERENCES

1. Kissi, M. S., T. Kumpuniemi, et al., "Directive low-band UWB antenna for in-body medical communications," *IEEE Access*, Vol. 7, 149026–149038, 2019.
2. Khaleghi, A., I. Balasingham, and A. Vosoogh, "A compact ultra-wideband spiral helix antenna for in-body communications," *The 8th European Conference on Antennas and Propagation (EuCAP 2014)*, IEEE, 2014.
3. Miralles, E., C. Andreu, M. Cabedo-Fabrés, et al., "UWB on-body slotted patch antennas for in-body communications," *2017 11th European Conference on Antennas and Propagation (EUCAP)*, IEEE, 2017.
4. Godeneli, K., U. Bengi, O. A. Kati, et al., "A wearable dual-mode repeater antenna for implant communications," *IEEE Transactions on Antennas and Propagation*, Vol. 70, No. 2, 868–875, 2022.
5. Tak, J., K. Kwon, S. Kim, et al., "Dual-band on-body repeater antenna for in-on-on WBAN applications," *International Journal of Antennas and Propagation*, Vol. 2013, No. 107251, 2013.
6. Magill, M. K., G. A. Conway, and W. G. Scanlon, "Circularly polarized dual-mode wearable implant repeater antenna with enhanced into-body gain," *IEEE Transactions on Antennas and Propagation*, Vol. 68, No. 5, 3515–3524, 2020.
7. Xu, L. J., Z. Duan, Y. M. Tang, and M. Zhang, "A dual-band on-body repeater antenna for body sensor network," *IEEE Antennas and Wireless Propagation Letters*, Vol. 15, 1649–1652, 2016.